energies

MDPI

Article

Thermodynamic Modeling and Parameter Study of a Supercritical CO_2 Pneumatic Launch System for Sustainable High-Payload Applications

Gaoliang Liao [1,2,*,†], Zhong Liu [1,†], Feng Zhang [2] and Jiaqiang E [2]

[1] Guangxi Key Laboratory of Special Engineering Equipment and Control, Guilin University of Aerospace Technology, Guilin 541004, China
[2] College of Mechanical and Vehicle Engineering, Hunan University, Changsha 410082, China
* Correspondence: liaogaoliang@hnu.edu.cn
† These authors contributed equally to this work.

Abstract

This study develops and validates a thermodynamic model for a supercritical carbon dioxide (CO_2) pneumatic launch system, evaluating its potential as an environmentally friendly and efficient energy conversion technology alternative to conventional working fluids such as compressed air and nitrogen. Utilizing real-gas thermophysical properties from the NIST database, the model incorporates mass and energy conservation principles to simulate the transient launch process. Under the assumption of a pre-attained initial state, comparative analyses demonstrate that supercritical CO_2 offers significantly higher specific internal energy, resulting in up to 20% greater payload capacity and improved exit velocities under identical initial conditions. A detailed parametric investigation examines the effects of key structural parameters—including the initial volume of the low-pressure chamber, launch tube diameter, valve diameter, and valve opening time—on launch performance, efficiency, and safety. Results indicate that while a smaller low-pressure chamber volume and larger launch tube diameter enhance launch efficiency and velocity, they must be balanced against structural safety limits to avoid excessive acceleration. Valve diameter expansion improves mass transfer and acceleration, yet diminishing returns are observed beyond 0.10 m. The study highlights supercritical CO_2 as a promising high-energy-density working fluid that eliminates toxic exhaust at the launch site. These findings provide practical guidelines for system design optimization, offering a technical pathway toward compact, low-emission pneumatic launch equipment, provided that the upstream energy for CO_2 conditioning is efficiently managed.

Keywords: supercritical carbon dioxide; pneumatic launch; real-gas model; parametric analysis; launch performance; thermodynamic modeling

Check for updates

Academic Editor: Jan Taler

Received: 26 December 2025
Revised: 15 January 2026
Accepted: 21 January 2026
Published: 22 January 2026

Copyright: © 2026 by the authors. Licensee MDPI, Basel, Switzerland. This article is an open access article distributed under the terms and conditions of the Creative Commons Attribution (CC BY) license.

1. Introduction

Pneumatic launch, as a representative cold launch technology, has been extensively investigated for military and aerospace industries, such as aircraft launch [1–4], rocket launch [5,6] and cannon launch [7]. In this context, "cold launch" is operationally defined as a propulsion process that excludes chemical combustion within the launch tube, thereby eliminating high-temperature flame erosion and luminous plumes during the firing sequence. Using compressed gas as the working medium, this technology offers advantages including zero pollution, low infrared signatures, and high reusability. Traditionally, steam

has been the primary medium due to its technological maturity [8]. However, a critical evaluation of steam-based systems reveals inherent bottlenecks: the reliance on intricate piping and massive auxiliary systems inevitably leads to a large spatial footprint and excessive weight. Moreover, the extreme operational temperature (up to 1000 K) and limited adjustability of launch force pose significant challenges for precision control and system durability [9–12].

To overcome these structural complexities, research has shifted toward compressed air and nitrogen, which offer more compact architectures. While both media posses comparable specific internal energy, a comparative analysis shows that nitrogen requires costly extraction and purification processes, making compressed air a more economically viable candidate for large-scale implementation. Consequently, a large body of research has focused on optimizing compressed air launch performance. A key academic focus in this area is the accurate characterization of gas behavior under high pressure. For instance, Ren et al. [2] and Peng et al. [13] have debated the efficacy of various equations of state (EOS), revealing that while the P = R and S-R-K equations are standard, they may lack the precision required for a high-pressure pneumatic pilot-driven system compared to improved virial equations. Furthermore, while studies by Jin et al. [14] and Sung et al. [15] have identified the impact of structural parameters and compression waves on muzzle velocity, these air-based systems remain constrained by a fundamental thermodynamic limitation: the relatively low specific internal energy of air/nitrogen necessitates prohibitively large storage tanks, typically restricting their payload capacity to projectiles under 500 pounds [16].

This energy density gap has prompted the exploration of alternative media with superior thermophysical properties. As illustrated in Figure 1, the specific internal energy of carbon dioxide (CO_2) significantly exceeds that of nitrogen and air within the 300–400 K range. Crucially, the proximity of CO_2's critical point (T_{cr} = 304.13 K, P_{cr} = 7.37 MPa) to ambient conditions suggests that supercritical CO_2 can provide a high-energy-density state without the thermal overhead of steam.

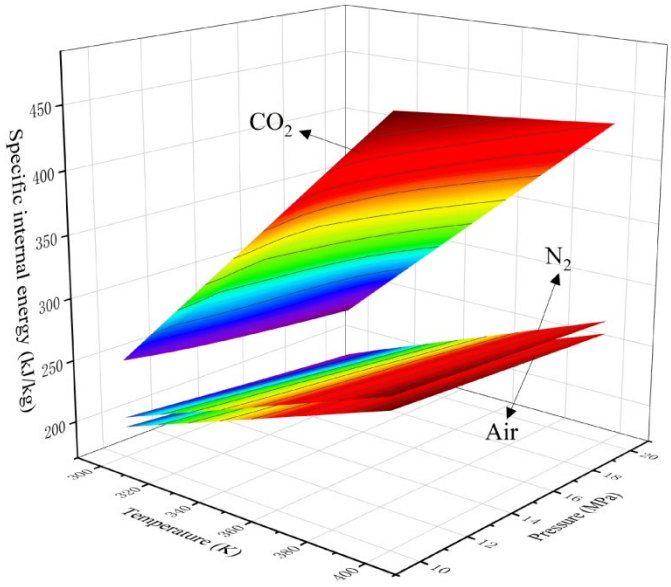


Figure 1. Specific internal energy for different gases [17].

Recent preliminary studies have begun to testify the feasibility of supercritical CO_2 launch, yet a comprehensive theoretical framework is still evolving. While Yao et al. [1] and Wang et al. [3] identified that launch success is highly sensitive to valve control strategies and initial chamber conditions, these studies often focus on specific operational parameters rather than the underlying thermodynamic efficiency gains compared to traditional media.

Although Wen et al. [18] indicated a potential 50% increase in payload capacity, there remains a lack of integrated models that simultaneously account for real-gas thermophysical property fluctuations and a broad spectrum of structural sensitivities.

As mentioned above, supercritical CO_2 pneumatic launch has been considered as a potential launch technology in military and aerospace industries. Compared with steam and compressed air, there has been relatively limited research on supercritical CO_2 pneumatic launch. However, although several studies exist, systematic parametric and transient thermodynamic analyses for supercritical CO_2 pneumatic launch under real-gas conditions remain limited. Given these gaps, the present study develops a robust thermodynamic model based on mass and energy conservation, incorporating the precise thermophysical properties of real gases. Unlike previous works that treat media in isolation, this research presents a comparative investigation into the launch efficiency of different working mediums. Additionally, the coupled effects of structural parameters—including low-pressure chamber volume, tube diameter, and valve dynamics—on launch performance are discussed in detail to provide a theoretical basis for sCO_2 pneumatic launch system design. Finally, the main conclusions of this study are summarized.

2. Mathematical Model

A schematic diagram of the pneumatic launch system is illustrated in Figure 2. The pneumatic launch system primarily consists of a high-pressure chamber, a control valve, a low-pressure chamber, a piston, a projectile which may refer to an aircraft, missile, or cannon, and a launch tube. At the launch readiness state, liquid carbon dioxide in the high-pressure chamber is heated to a supercritical state ($T > 304.13$ K, $P > 7.37$ MPa). There are various methods for heating carbon dioxide, such as chemical ignition or electric heating. This study focuses primarily on the launch performance of a supercritical CO_2 pneumatic launch system. The CO_2 heating process is not considered here, as it is assumed that CO_2 inside the high-pressure chamber has already reached the designated initial state at the time of launch. Therefore, the scope of this numerical simulation is strictly confined to the "launch event"—the transient period from valve opening to projectile exit—rather than the entire preparation and thermal conditioning cycle. Once the pressure of supercritical CO_2 reaches the preset value, the valve assemblies between the high-pressure and low-pressure chamber are opened in a specific sequence. The supercritical CO_2 from the high-pressure chamber then rapidly expands as it enters the low-pressure chamber, performing work by driving the projectile to accelerate. This continues until the projectile exits the launch tube at a certain velocity, thereby completing the launch process.

The flow of the supercritical CO_2 behind the projectile in the launch tube is a complex and transient process [14,19,20]. To simplify the mathematical model while maintaining computational tractability, the following assumptions are utilized:

(1) The supercritical CO_2 is uniformly distributed in the high-pressure and low-pressure chamber, and it is in a state of thermal equilibrium at any time.
(2) Due to the short duration of the launch process, the heat exchange between the pneumatic launch system and the ambient environment is neglected. (Adiabatic assumption for the entire system).
(3) The expansion of supercritical CO_2 within the high-pressure and low-pressure chambers is treated as an isentropic process. However, the flow through the control valve is considered an irreversible throttling process, where the irreversibility is accounted for by the flow coefficient.
(4) The supercritical CO_2 flow along the launch tube is a one-dimensional quasi-steady flow, and the influence of the ejection on projectile motion is not considered. While these simplifications neglect the complex transient shock wave reflections and the

air entrainment effects ahead of the projectile, they remain valid for evaluating the primary thermodynamic energy conversion within the subsonic and low-transonic regimes. The quasi-steady assumption is particularly applicable when the projectile velocity is significantly lower than the local speed of sound of the supercritical CO_2, and when the launch tube length-to-diameter ratio is within a range where localized wave dynamics do not dominate the base pressure distribution [15,17].

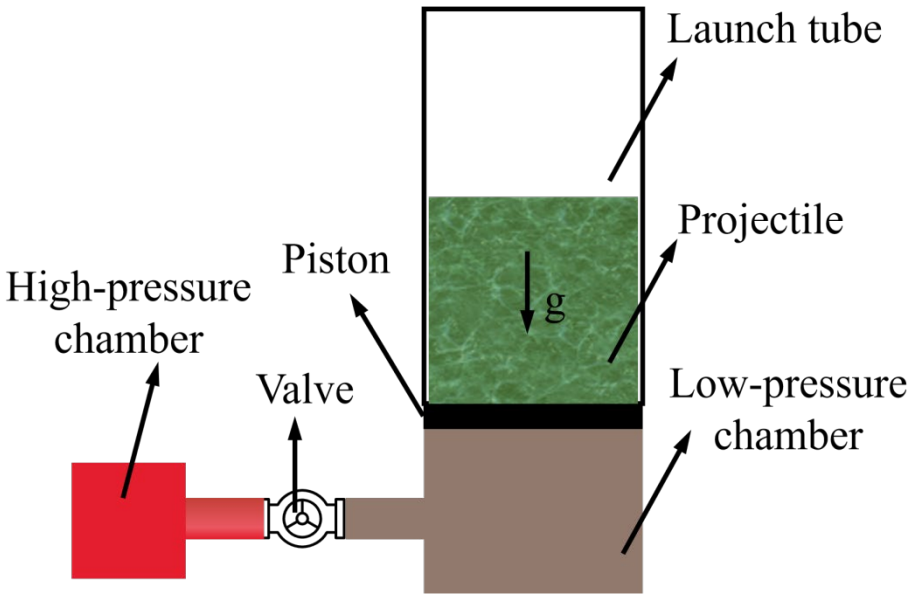


Figure 2. Schematic diagram of pneumatic launch system.

To account for the influence of real-gas effects, the thermophysical properties of the supercritical CO_2 in this study are obtained from the NIST database [17]. As the supercritical CO_2 flows through the valve from the high-pressure chamber into the low-pressure chamber, both of which are sealed, the mass decrease in the high-pressure chamber equals the mass increase in the low-pressure chamber and is equal to the mass flow rate through the valve. The mass flow rate through the valve is determined based on whether choked flow occurs. It should be noted that while the fluid inside the chambers follows isentropic relations, the transition through the valve involves dominant irreversibilities due to turbulence and friction. In this model, these non-ideal effects are lumped into the flow coefficient (C_d), which represents the deviation from ideal isentropic flow through the orifice [21]

$$q_m = \begin{cases} C_d \cdot A_{val} \cdot \sqrt{\frac{2k}{k-1} \cdot P_{HP}\rho_{HP} \cdot \left(\left(\frac{P_{LP}}{P_{HP}}\right)^{\frac{2}{k}} - \left(\frac{P_{LP}}{P_{HP}}\right)^{\frac{k+1}{k}} \right)} & \frac{P_{LP}}{P_{HP}} > \left(\frac{2}{k+1}\right)^{\frac{k}{k-1}} \\ C_d \cdot A_{val} \cdot \sqrt{k \cdot P_{HP}\rho_{HP} \cdot \left(\frac{2}{k+1}\right)^{\frac{k+1}{k-1}}} & \frac{P_{LP}}{P_{HP}} \le \left(\frac{2}{k+1}\right)^{\frac{k}{k-1}} \end{cases} \quad (1)$$

where C_d denotes the flow coefficient with a range of 0.85~0.95. A_{val} is the valve and k is the isentropic coefficient. P and ρ are the pressure and density. Subscripts of HP and LP, respectively, present the high-pressure chamber and low-pressure chamber.

When the supercritical CO_2 enters the low-pressure chamber, it performs work once the driving force exceeds the resistances. The initiation criterion for projectile motion is determined by the balance of the following forces: the driving force from P_{LP}, the opposing atmospheric pressure force, the mass force of the piston and the projectile, and the static

frictional resistance. Compared to the projectile, the weight of the piston is negligible. The threshold condition is expressed as

$$\frac{dv}{dt} = \frac{(P_{LP} - P_0) \cdot A_{pis} - m_p \cdot g \cdot \left(1 + C_f\right)}{m_p} \text{ when } P_{LP} > P_0 + \frac{g m_p}{A_{pis}} \tag{2}$$

where g represents the gravitational acceleration, v is the launch velocity, P_0 is the atmospheric pressure, m_p is the projectile mass, and C_f is the friction coefficient between the projectile and launch tube.

When supercritical carbon dioxide flows out the high-pressure chamber and performs work in the low-pressure chamber as the projectile is launched, gas–liquid phase transition may occur, resulting in a gas–liquid equilibrium state. Under the circumstances, an iterative calculation is required to determine the mass fractions of gaseous CO_2 and liquid CO_2. Taking the high-pressure chamber as an example, the mass and total internal energy could be obtained based on the mass and energy conservation (as shown in Equations (3) and (4)). Then, the density (ρ_{HP}) and specific internal energy (u_{HP}) at the current iteration step can be calculated from the mass, total internal energy, and volume of the high-pressure chamber. Subsequently, assuming a pressure value for the high-pressure chamber, the pressure and temperature of both the gas and liquid phases are equal to the system pressure and temperature if the system is in a two-phase equilibrium state. Combined with Equations (5)–(7), the actual pressure value could be obtained through iterative calculation.

$$\frac{dm_{HP}}{dt} = -q_m \tag{3}$$

$$\frac{dU_{HP}}{dt} = -q_m \cdot h_{HP} \tag{4}$$

$$x_v + x_l = 1 \tag{5}$$

$$\frac{1}{\rho_{HP}} = \frac{x_v}{\rho_{v,sat}} + \frac{x_l}{\rho_{l,sat}} \tag{6}$$

$$u_{HP} = x_v \cdot u_{v,sat} + x_l \cdot u_{l,sat} \tag{7}$$

For the low-pressure chamber, the mass and energy balances must account for the dynamic volume expansion as the projectile moves. The governing equations are expressed as

$$\frac{dm_{LP}}{dt} = q_m \tag{8}$$

$$\frac{d\left(m_{Lp} u_{LP}\right)}{dt} = q_m \cdot h_{HP} - \frac{d(E_k + E_p)}{dt} - \frac{d\left(P_0 A_{pis} L + g m_p L\right)}{dt} \tag{9}$$

$$V_{LP} = V_{LP,0} + A_{pis} L \tag{10}$$

$$\frac{dL}{dt} = v \tag{11}$$

where E_k and E_p are, respectively, the kinetic energy and potential energy of the projectile, L is the projectile displacement, and $V_{LP,0}$ is the initial volume of the low-pressure chamber.

In addition to the launch velocity and acceleration, the mass transfer efficiency (η_{MT}) and launch efficiency (η_{LE}) are introduced to evaluate the launch process under different conditions. The mass transfer efficiency is defined as the ratio of the mass decrement to the initial mass in the high-pressure chamber, which is written as:

$$\Delta_{MT} = \frac{\Delta m_{HP}}{m_{0,HP}} \tag{12}$$

The launch efficiency is defined as the ratio of the projectile kinetic energy and potential energy to the high-pressure chamber initial total internal energy. It should be noted that this parameter represents the pneumatic conversion efficiency of the stored internal energy during the expansion event. It does not account for the energy consumed during the pre-launch heating phase, which would be required for a full-cycle thermoeconomic evaluation. It can be written as:

$$\eta_{LE} = \frac{E_k + E_p}{U_{0,HP}} \tag{13}$$

In this paper, the time-discretization method is employed to solve the aforementioned differential equations. Judicious selection of the time step is essential for the reason that the time step size has a significant impact on the computation time and prediction accuracy. Five different time steps, such as 1×10^{-4} s, 5×10^{-4} s, 1×10^{-3} s, 5×10^{-3} s, and 1×10^{-2} s, are selected to analyze the effect of time step on the launch performance (as shown in Figure 3). It can be seen that when the time step is smaller than 1×10^{-3} s, its influence on the launch velocity can be neglected. Therefore, a time step of 1×10^{-3} s is adopted for subsequent calculations.

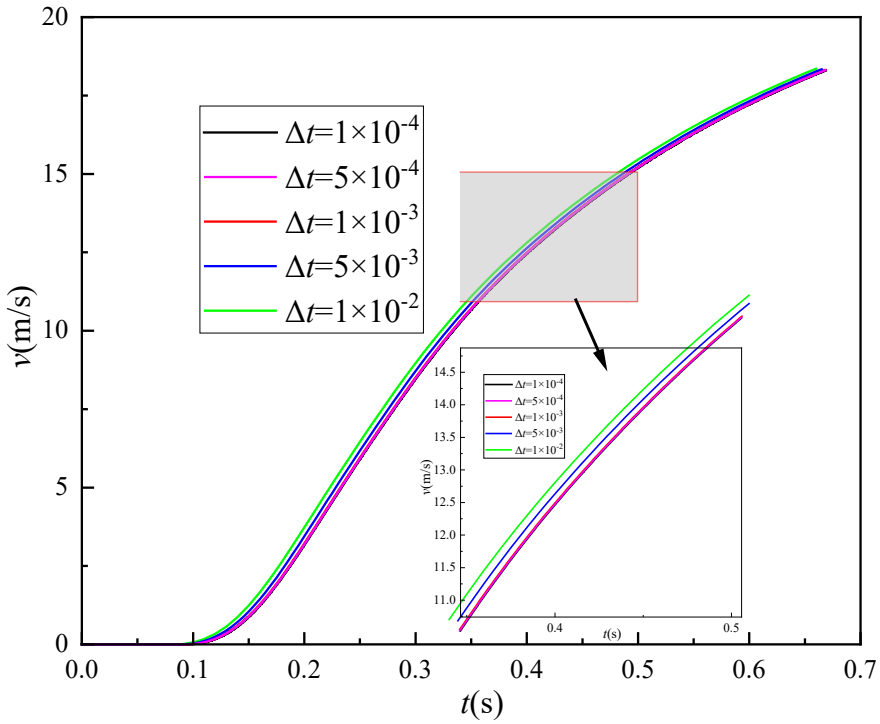


Figure 3. Effect of time step on the launch performance.

While the developed mathematical model facilitates an efficient evaluation of supercritical CO_2 pneumatic launch performance, several physical limitations and underlying assumptions must be acknowledged to define its applicable boundaries:

(1) The model adopts a lumped-parameter approach (Assumption 1), assuming uniform thermophysical properties within the chambers. However, in practical high-pressure launch scenarios, the rapid expansion of supercritical CO_2 can trigger complex unsteady wave phenomena, such as expansion waves and potential shock reflections. These spatial gradients, which could influence the instantaneous pressure distribution on the projectile base, are not captured by the current one-dimensional quasi-steady flow assumption.

(2) Although the adiabatic assumption (Assumption 2) is justified by the millisecond-scale duration of the launch, the extreme thermodynamic state of supercritical CO_2

near its critical point may lead to localized high heat-transfer coefficients. Neglecting the convective heat exchange between the fluid and the cylinder walls might result in a slight overestimation of the expansion work and the final muzzle velocity.

(3) The mechanical friction is treated using a constant coefficient (C_f), which does not account for the dynamic changes in lubrication conditions or the thermal expansion of seals during high-speed motion. Furthermore, the model assumes a perfect seal, while gas leakage through the clearance between the projectile and the launch tube could lead to pressure loss in engineering practice.

3. Results and Discussions

3.1. Model Validation

Wang et al. [3] established a supercritical CO_2 pneumatic test platform, consisting of a high-pressure chamber, a low-pressure chamber, and a valve connecting the two chambers. Based on the mathematical model described above, a simulation mode for the supercritical CO_2 pneumatic system identical to that described in Ref. [3] is used. A comparison of the simulated pressure and experimental value in the high-pressure chamber is shown in Figure 4. It can be seen that the simulation and experiment show good consistency in the state parameter of supercritical CO_2, verifying the correctness of the mathematical model.

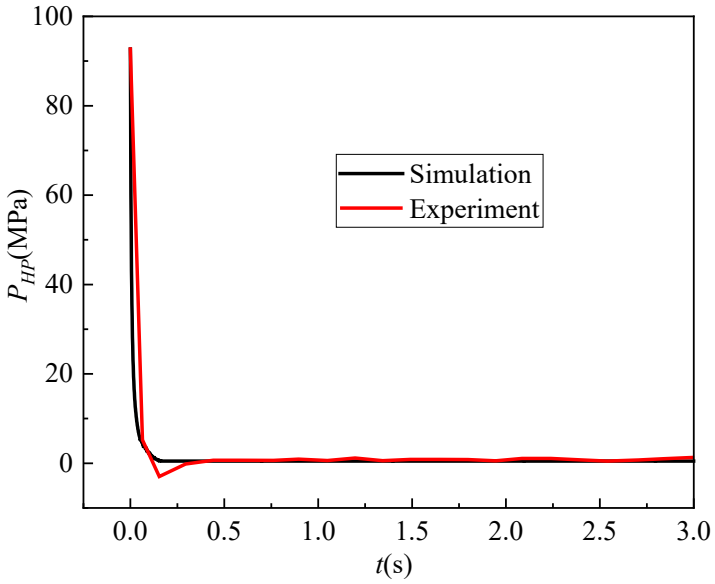


Figure 4. Comparison of the simulation and experiment.

3.2. Effect of Different Working Mediums

In this section, the comparison between supercritical CO_2, air and nitrogen (N_2) is conducted under identical initial conditions (same P_0, T_0, V_0). It is important to acknowledge that due to the significantly higher density of supercritical CO_2 near the critical point, this comparative criterion implies a larger initial mass and a higher total stored energy inventory for the supercritical CO_2 system. However, from an engineering and structural perspective, the maximum pressure and the physical volume are the primary design constraints of launch platforms. By demonstrating that supercritical CO_2 delivers superior performance within the same spatial and structural limits, this study highlights its potential for system miniaturization and payload enhancement, even though the total energy inventory differs. The volume of the high-pressure chamber is 0.1 m^3. The valve diameter is 0.1 m and the flow coefficient is set as 0.9. The initial volume of the low-pressure chamber is 1 m^3. The launch tube has an diameter of 0.3 m and a length of 6.0 m. The initial

states of the high-pressure chamber and low-pressure chamber are, respectively, 12 MPa and 350 K, and 0.1 MPa and 293.15 K.

Figure 5 shows the variation in velocity and acceleration over time with a projectile of 600 kg. When the pressure in the low-pressure chamber becomes sufficient to overcome the combined weight of the piston and the projectile, atmospheric pressure, and frictional resistance, the projectile starts its motion. Compared with the air and N_2, the pneumatic launch using CO_2 as the working medium exhibits a slightly delayed initiation. The initiation time of the projectile under different working mediums is 0.106 s, 0.092 s, and 0.091 s for CO_2, air, and N_2, respectively. Following the initiation of the projectile's motion, the acceleration under a different working medium displays a similar variation pattern, which first increases to a peak value and then gradually decreases until the projectile exits the launch tube. The maximum acceleration for CO_2, air, and N_2 is, respectively, 72.54 m/s^2, 69.73 m/s^2, and 69.27 m/s^2. Due to the delayed initiation, the projectile velocity with CO_2 is initially lower than that with air or nitrogen, but subsequently exceeds it. The projectile finally leaves the launch tube at a maximum velocity of 27.22 m/s, 25.25 m/s, and 25.14 m/s for CO_2, air, and N_2, respectively.

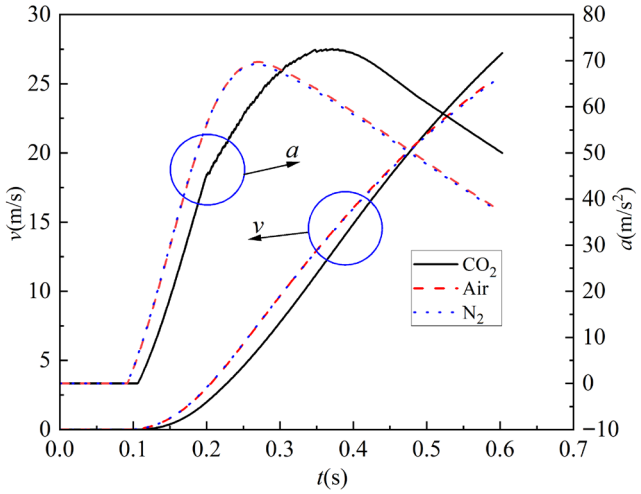


Figure 5. Time curves of velocity and acceleration with a projectile of 600 kg.

While maintaining the initial state parameters and the volumes of the high-pressure and low-pressure chamber constant, the effects of the projectile mass on the exit velocity and maximum acceleration under different working mediums are illustrated in Figure 6. As the projectile mass increases, the exit velocity and acceleration of the projectile decrease. It can be seen that when the projectile mass is the same, the exit velocity and acceleration using CO_2 are higher than that with air or N_2. Moreover, the difference in the exit velocity and acceleration between CO_2 and either air or N_2 slightly widens with the increase in the projectile mass. For the same exit velocity, such as 22 m/s, the supercritical CO_2 pneumatic device can launch a projectile of 1200 kg, whereas using air or N_2 allows only a 1000 kg projectile to be launched. Compared to air or N_2, the supercritical CO_2 pneumatic launch could obtain a 20% increase in payload mass. The increase in payload capacity using supercritical CO_2 can be attributed to its unique thermodynamic behavior during expansion, specifically the real-gas effect near the critical point. Unlike air or N_2, which behave similarly to ideal gases where the pressure drops rapidly as volume increases, supercritical CO_2 exhibits a lower adiabatic expansion exponent in the supercritical and high-pressure liquid–gas transition regions. In the energy balance equation (Equation (9)), the internal energy term u_{LP} of supercritical CO_2 is less sensitive to volume expansion compared to air. This results in a "flatter" pressure decay curve behind the projectile, meaning

the supercritical CO_2 maintains a higher base pressure throughout the launch stroke. Consequently, the integral work is significantly larger for supercritical CO_2, providing the sustained energy required to accelerate heavier payloads to the same exit velocity.

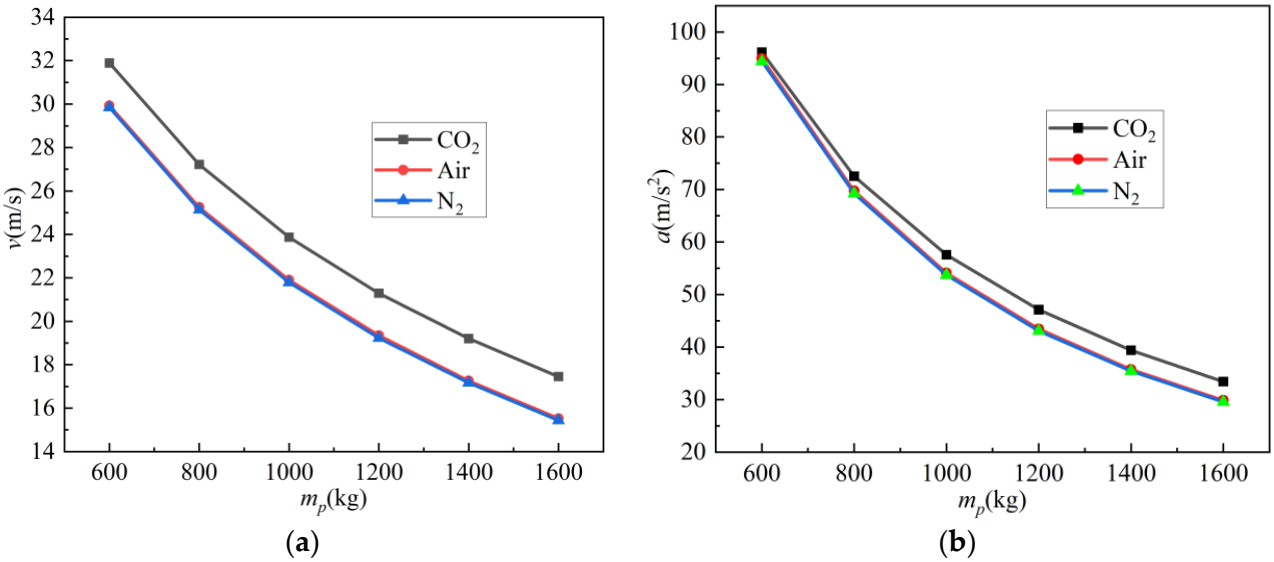


Figure 6. Projectile mass variations in the velocity (**a**) and acceleration (**b**).

3.3. Effect of Structural Parameters

In order to elucidate the governing laws affecting the performance of the supercritical CO_2 pneumatic launch, the effect of structural parameters, including the initial volume of the low-pressure chamber, launch tube diameter, valve diameter, and valve opening time, are investigated in this section. The initial states of the high-pressure chamber and low-pressure chamber are, respectively, 12 MPa and 350 K, and 0.1 MPa and 293.15 K. The projectile mass is 1000 kg and the volume of the high-pressure chamber is 0.1 m^3.

Five initial volumes of the low-pressure chamber, specifically 0.2 m^3, 0.4 m^3, 0.6 m^3, 0.8 m^3, and 1.0 m^3, are selected to investigate the effect on the pneumatic launch process. Figure 7 presents the motion parameter of the projectile during the launch process. With the increase in the initial volume of the low-pressure chamber, the launch time represented as the duration the projectile remains inside the launch tube gradually increases. The launch time increases from 0.408 s for a 0.2 m^3 initial volume to 0.664 s for 1.0 m^3, representing a 62.7% increase. This can be attributed to the decreasing rate of pressure buildup in the low-pressure chamber as the initial volume increases. As shown in Figure 7, both the exit velocity and maximum acceleration for the projectile decrease with the increase in the initial volume of the low-pressure chamber. Considering the structural stability of the projectile during the launch process, a peak acceleration limit of 80 m/s^2 is adopted in this study as a safe constraint according to Ref. [1]. Consequently, a smaller initial volume of the low-pressure chamber is not always preferable. Comprehensive consideration of both the structural safety and launch velocity is required.

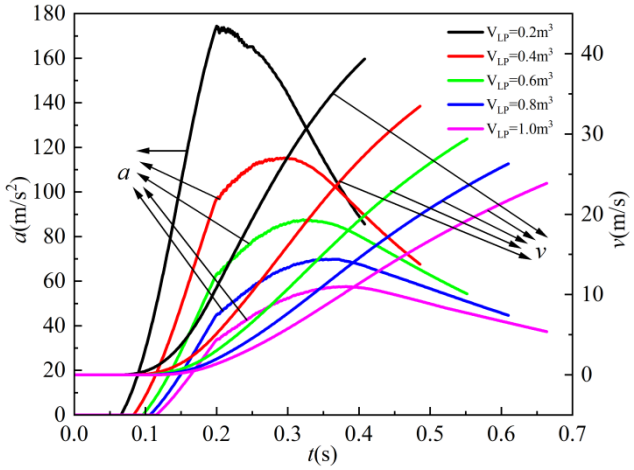


Figure 7. Variation in velocity and acceleration under different initial volumes of low-pressure chambers.

Figure 8 shows the changes in both the launch efficiency (η_{LE}) and mass transfer efficiency (η_{MT}) with different initial volumes of the low-pressure chamber. The mass transfer efficiency reflects the extent to which CO_2 from the high-pressure chamber actually enters the low-pressure chamber. During the launch process, most of the energy remains stored in the low-pressure chamber. As a result, the proportion of kinetic and potential energy in the projectile is relatively low, indicating low launch efficiency. This explains why the launch efficiency remains in the single-digit percentage range, while the mass transfer efficiency can exceed 90%, as shown in Figure 8. Additionally, as the initial volume of low-pressure chamber increases, the launch efficiency decreases, while the mass transfer efficiency increases. It can be concluded that a smaller initial volume of the low-pressure chamber should be selected to ensure a higher launch efficiency.

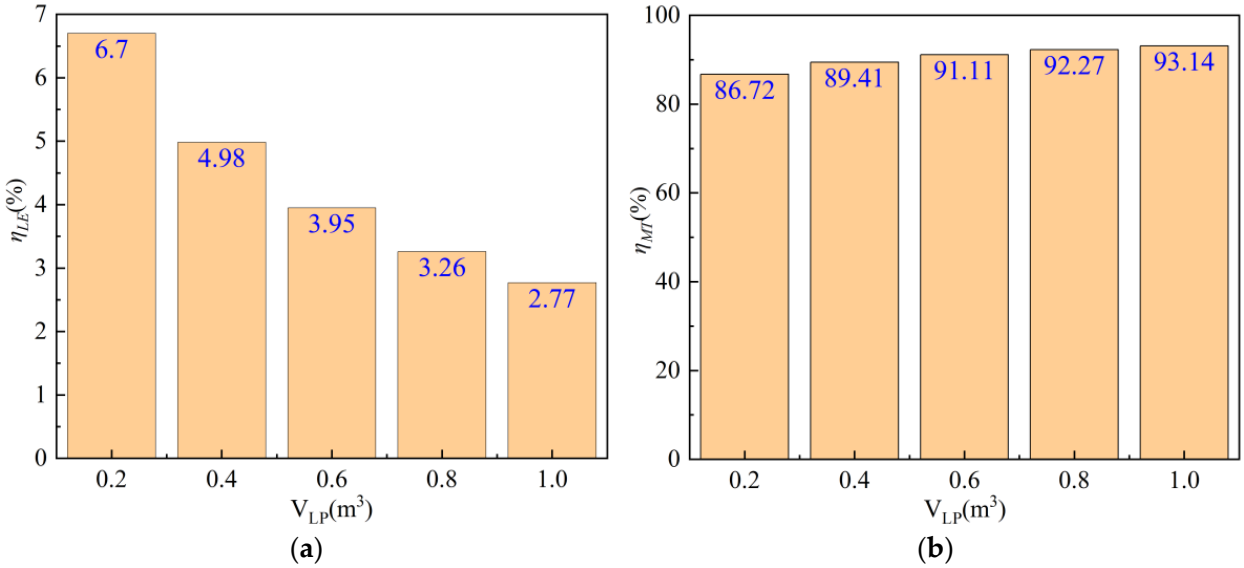


Figure 8. Initial volume variations in the launch efficiency (**a**) and mass transfer efficiency (**b**).

The effect of launch tube diameter on the velocity and acceleration of the projectile in the launch process is illustrated in Figure 9. When the launch tube diameter varies from 0.25 m to 0.45 m, the projectile exit velocity increases from 19.68 m/s to 32.66 m/s, representing a 66% increase. Nevertheless, as the launch tube diameter exceeds 0.35 m, the corresponding maximum acceleration during the launch process surpasses the limit

of 80 m/s^2. Therefore, to ensure the structural safety and stability of the projectile during the launch process, the launch tube diameter should not exceed 0.35 m. Figure 10 shows the variation in launch efficiency and mass transfer efficiency with respect to the launch tube diameter. As the launch tube diameter increases, the launch efficiency improves significantly, while the mass transfer efficiency shows little variation.

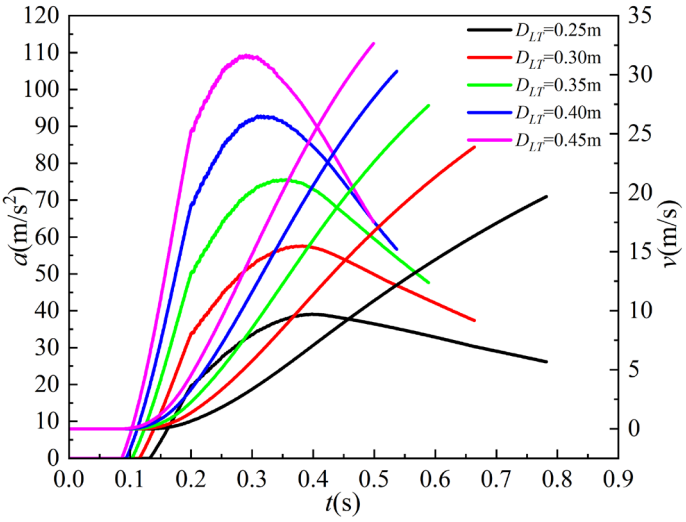


Figure 9. Variation in velocity and acceleration under different diameters of launch tube.

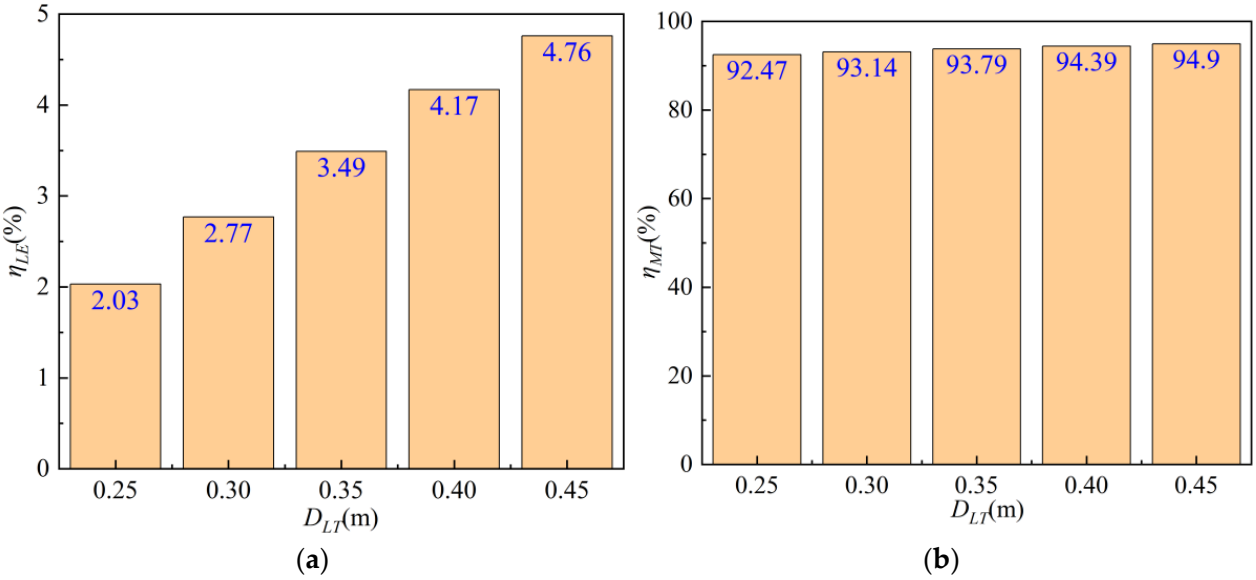


Figure 10. Tube diameter variations in the launch efficiency (**a**) and mass transfer efficiency (**b**).

In order to investigate the influence of valve diameter on the performance of supercritical CO_2 pneumatic launch, a comparative analysis is conducted on the effects of six different valve diameters on the projectile motion characteristics, launch efficiency and mass transfer efficiency. As shown in Figure 11, as the valve diameter increases from 0.05 m to 0.10 m, the launch time decreases from 0.87 s to 0.664 s, representing a reduction of 23.7%. An increase in valve diameter is beneficial for improving the mass transfer efficiency (as presented in Figure 12b), thereby resulting in higher acceleration (as shown in Figure 11). Correspondingly, the exit velocity of the projectile increases with the valve diameter, but the increase rate gradually diminishes. This indicates that further increases in valve diameter yield diminishing returns in terms of exit velocity improvement. Along with the changes in valve diameter, the launch efficiency follows a trend consistent with that of the exit velocity.

It can be shown from Figure 12a that, when the valve diameter increases from 0.05 m to 0.06 m, the relative improvement in launch efficiency is 12%; in contrast, when the valve diameter increases from 0.09 m to 0.10 m, the relative improvement drops to only 1.5%.

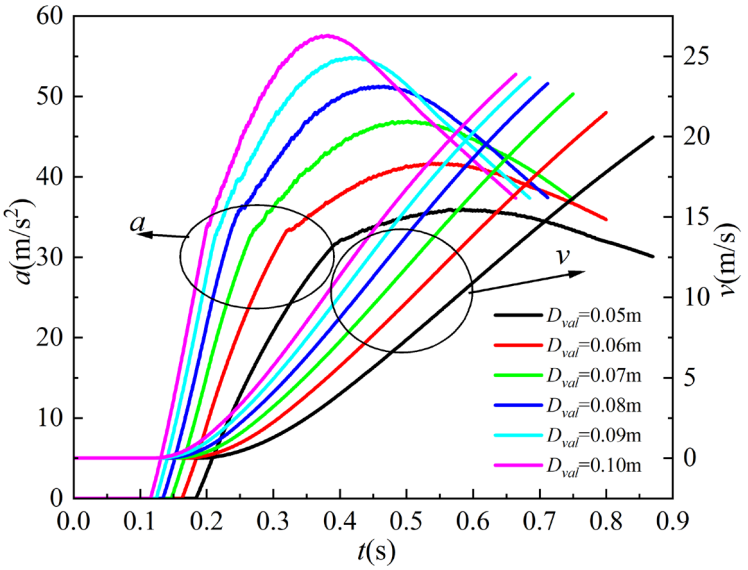


Figure 11. Variation in velocity and acceleration under different valve diameters.

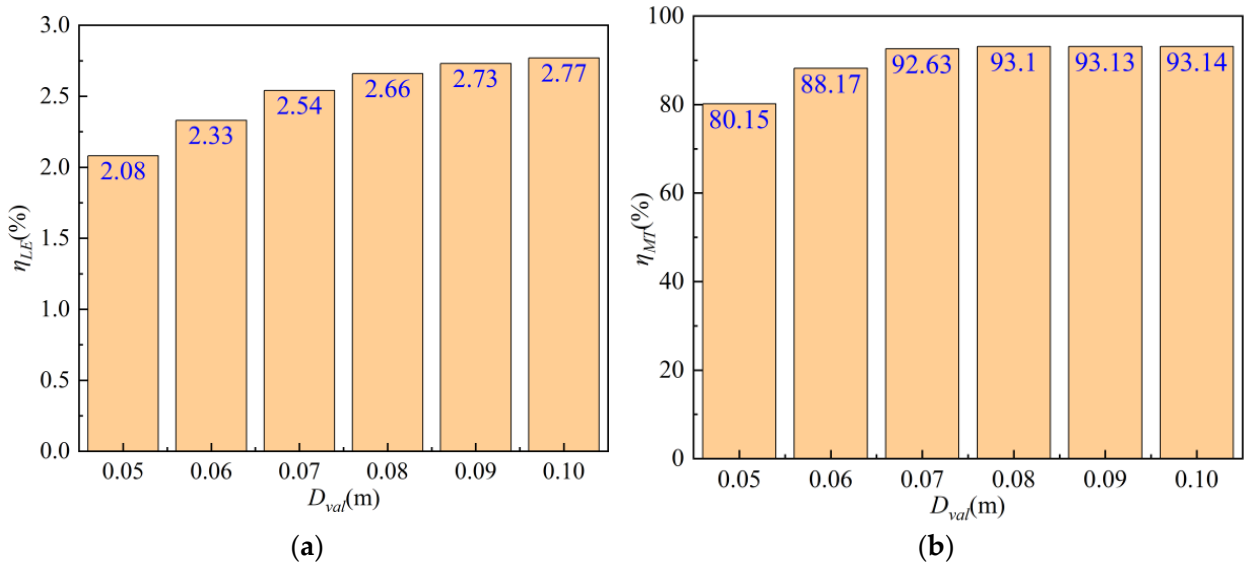


Figure 12. Valve diameter variations in the launch efficiency (**a**) and mass transfer efficiency (**b**).

In this paper, the valve opening follows an exponential function to achieve rapid actuation, which has a high initial slope, quickly approaching its maximum value. The valve opening function is expressed as

$$A = A_{val,\max} \cdot (1 - \exp(-1.27 \cdot t) \quad (14)$$

where $A_{val,max}$ is the full opening area of valve. The time corresponding to the full opening area is defined as the full opening time of valve. Figure 13 represents the effect of the full opening time of valve on the projectile velocity and acceleration in the launch process. As the full opening time of the valve increases, the exit velocity of the projectile remains largely unchanged while the launch time exhibits an increase. It can also be observed that the velocity and acceleration curves of the projectile shift entirely to the right with the increase

in full opening time of the valve. Consequently, the variations in launch efficiency and mass transfer with respect to valve opening time are negligible (as shown in Figure 14).

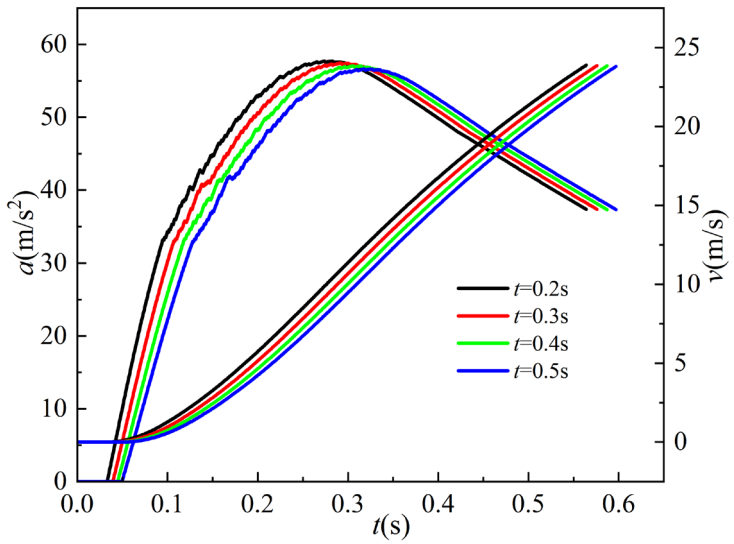


Figure 13. Variation in velocity and acceleration under different full opening times of valve.

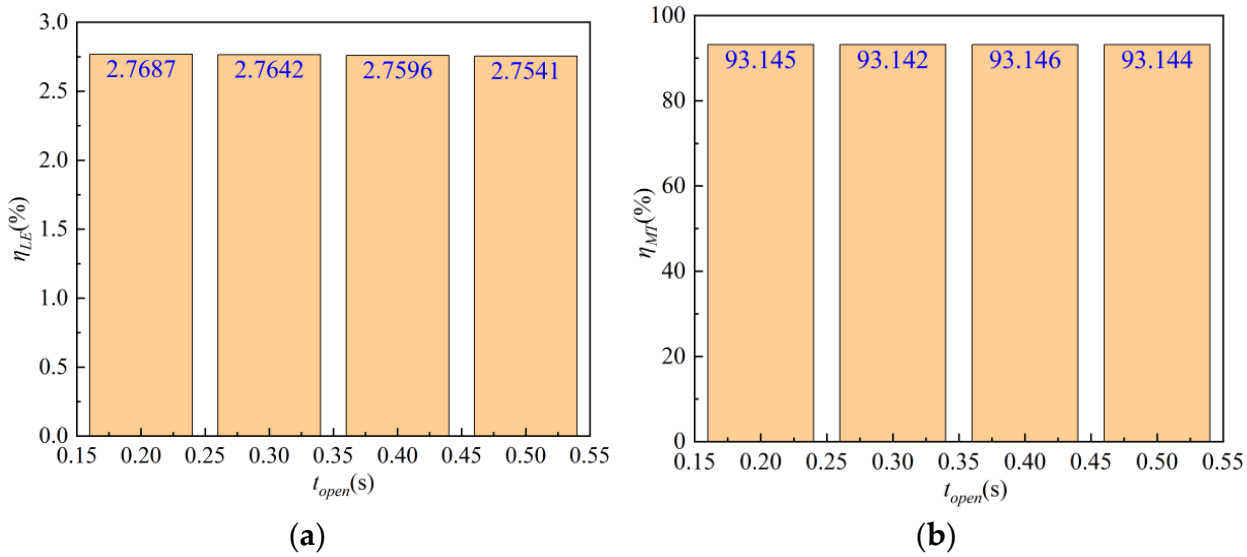


Figure 14. Valve opening time variations in the launch efficiency (**a**) and mass transfer efficiency (**b**).

4. Conclusions

This study developed and validated a thermodynamic model for supercritical CO_2 pneumatic launch systems, incorporating real-gas effects through NIST thermophysical data. The model was used to compare the performance of CO_2, air, and nitrogen as working mediums, demonstrating that supercritical CO_2 offers significantly higher specific internal energy, leading to improved launch velocities and payload capacity—up to 20% greater than air or nitrogen under comparable conditions.

Parametric investigations revealed that structural parameters critically influence launch performance. A smaller initial volume in the low-pressure chamber reduces launch time and increases acceleration, though it must be balanced against structural safety limits. Increasing the launch tube diameter enhances exit velocity and launch efficiency, but diameters exceeding 0.35 m may result in excessive acceleration beyond safe thresholds. Valve diameter expansion improves mass transfer and acceleration, yet benefits diminish

beyond 0.10 m, indicating an optimal design range. Valve opening time was found to have minimal impact on launch velocity and efficiency, suggesting that rapid valve actuation strategies are not performance-limiting.

In summary, supercritical CO_2 represents a promising working medium for high-performance pneumatic launch systems, particularly for heavy payloads. The insights from this parametric study provide practical guidelines for optimizing system design, balancing efficiency, safety, and structural feasibility. Future work may explore dynamic valve control strategies, two-phase flow effects, and experimental validation under varied operational conditions.

Author Contributions: Conceptualization, G.L., F.Z. and J.E.; Methodology, G.L.; Software, G.L.; Validation, G.L.; Investigation, G.L.; Writing—original draft, G.L.; Writing—review & editing, G.L., Z.L., F.Z. and J.E.; Visualization, G.L.; Supervision, Z.L., F.Z. and J.E. All authors have read and agreed to the published version of the manuscript.

Funding: This research was funded by the Natural Science Foundation of Hunan Province (Grant No. 2023JJ30117) and the Guangxi Key Laboratory of Special Engineering Equipment and Control, Guilin University of Aerospace Technology (Grant No. 2411KFYB01).

Data Availability Statement: The data presented in this study are available on request from the corresponding author. The data are not publicly available due to privacy restrictions.

Conflicts of Interest: The authors declare that they have no conflicts of interest regarding the publication of this paper.

References

1. Yao, H.X.; Wei, X.Z.; Ye, H. Supercritical carbon dioxide as a new working medium for pneumatic launch: A theoretical study. *Def. Technol.* **2021**, *17*, 1296–1306. [CrossRef]
2. Ren, J.; Yang, F.; Ma, D.; Le, G.; Zhong, J. Pneumatic performance study of a high pressure ejection device based on real specific energy and specific enthalpy. *Entropy* **2014**, *16*, 4801–4817. [CrossRef]
3. Wang, J.; Li, T.; Zhang, Z.; Yao, S.; Lu, Z. Effect of valve on ballistic performance in supercritical CO_2 pneumatic launch. *J. CO_2 Util.* **2023**, *75*, 102580. [CrossRef]
4. Li, C.; Wen, J.; Wang, S.; Li, Y. Thermodynamic analysis on rapid pressurization of supercritical CO_2 for pneumatic launch performance. *J. CO_2 Util.* **2021**, *53*, 101710. [CrossRef]
5. Zhao, Z.X.; Jiang, Y.; Jia, Q.M.; Niu, Y. Research on interior ballistics of catapult using high-pressure working medium. *Acta Armamentarii* **2022**, *43*, 1553–1564.
6. Yao, L.; Ma, D.W.; Ma, W.N.; Ren, J.; Zhong, J.L.; Wang, Z.L. Interior ballistics modeling and optimization of one-side ejection device with two-step cylinder. *Acta Armamentarii* **2017**, *38*, 466–475.
7. Zhang, F.; Liu, H.; Wu, Y.; Li, J.; Yu, H.; Wang, X.; Guo, B.; Yuan, Y. General design and thermodynamic analysis of a supercritical carbon dioxide cannon. *J. Therm. Sci.* **2021**, *30*, 123–132.
8. Glebocki, R.; Jacewicz, M. Simulation study of a missile cold launch system. *J. Theor. Appl. Mech.* **2018**, *56*, 901–913. [CrossRef]
9. Zhang, X.J.; Xu, Y.J.; Xu, J.; Sheng, Y.; Zuo, Z.; Liu, J.; Chen, H.; Wang, Y.; Huang, Y. Study on the performance and optimization of a scroll expander driven by compressed air. *Appl. Energy* **2017**, *186*, 347–358. [CrossRef]
10. Dai, H.; Yang, C.; Zhang, F.; Liao, G.; Zhang, B. Transient heat dissipation performance investigation on the battery thermal management system based on S-CO_2 immersion cooling. *Energy* **2025**, *318*, 134656. [CrossRef]
11. You, M.; Feng, M.; Zhang, F.; Liao, G. Numerical investigation on the unsteady flow and coupled heat transfer characteristics between supercritical carbon dioxide and pulsating flow of water within a PCHE under offshore conditions. *Int. Commun. Heat Mass Transf.* **2026**, *172*, 110249.
12. Gao, Y.; Wang, C.; Sun, Y.B. Design, fabrication, and experimental study of a full-scale compressed air ejection system based on missile acceleration limitation. *Aerosp. Sci. Technol.* **2023**, *141*, 108519. [CrossRef]
13. Peng, Z.; Xu, Q.; Yang, C.H.; Ma, W.; Zhang, Z. Simulation and experimental investigation of high-pressure pneumatic pilot-driven on/off valve with high transient performances for compressed air ejection. *Flow Meas. Instrum.* **2023**, *94*, 102466.
14. Jin, Y.; Gu, Y.F.; Zhu, H.J.; Jiang, C.; Huang, J.; Zhu, J.; Zhu, Y. Launch dynamic simulation of a compressed-air launcher for fire suppression. *Appl. Sci.* **2023**, *13*, 9615. [CrossRef]

15. Sung, W.; Kim, J.; Jang, K.S.; Le, T.T.G.; Kim, J.; Kim, D.H.; Lee, H.; Ryu, J. Parametric study of a projectile launched by a compressed air cannon. *J. Mech. Sci. Technol.* **2023**, *37*, 5913–5933. [CrossRef]
16. Fahlstrom, P.; Gleason, T. *Introduction to UAV Systems*; John Wiley & Sons: Hoboken, NJ, USA, 2012.
17. National Institute of Standards and Technology. Thermophysical Properties of Fluid Systems. 2021. Available online: https://webbook.nist.gov/chemistry/fluid/ (accessed on 1 October 2025).
18. Wen, J.; Li, C.L.; Wang, Y.Y.; Zhao, X.; Wang, S.M.; Li, Y.Z. Feasibility analysis of CO_2 used in pneumatic catapult. *J. Astronaut.* **2021**, *42*, 1335–1342.
19. Lin, J.; Zhang, X.; Zhu, Y.; Liu, W. The technique of three-stage compressed-gas gun for hypervelocity impact. *Explos. Shock. Waves* **2012**, *32*, 483–489.
20. Hammer, M.; Ervik, A.; Munkejord, S.T. Method using a density-energy state function with a reference equation of state for fluid-dynamics simulation of vapor-liquid-solid carbon dioxide. *Ind. Eng. Chem. Res.* **2013**, *52*, 9965–9978.
21. Payri, R.; Gimeno, J.; Marti, A.P.; Martinez, M. Transient nozzle flow analysis and near field characterization of gasoline direct fuel injector using large eddy simulation. *Int. J. Multiph. Flow* **2022**, *148*, 103920. [CrossRef]

Disclaimer/Publisher's Note: The statements, opinions and data contained in all publications are solely those of the individual author(s) and contributor(s) and not of MDPI and/or the editor(s). MDPI and/or the editor(s) disclaim responsibility for any injury to people or property resulting from any ideas, methods, instructions or products referred to in the content.